AN ELECTROSTATIC MEASURING TECHNIQUE FOR MONITORING PARTICLE SIZE IN DILUTE PNEUMATIC TRANSPORT

by

Igor KUŠTRIN[a], Boštjan JURJEVČIČ[b], and Andrej SENEGAČNIK[a*]

[a] Faculty of Mechanical Engineering, University of Ljubljana, Ljubljana, Slovenia
[b] Adriaplin, Ljubljana, Slovenia

Original scientific paper
https://doi.org/10.2298/TSCI190417332K

The goal of this research is to establish the applicability of an electrostatic measuring technique for monitoring the quality of a coal-milling process in direct-firing systems. Such systems are used in large steam boilers fired with low-rank coal where the pulverized coal is transported pneumatically from the mills to the burner nozzles via ducts with large cross-sections. The electrostatic measuring method, in connection with intrusive rod-type sensors, was studied because it provides good spatial sensitivity and cost effectiveness. A laboratory test rig was constructed, where the pulverized coal carried by ambient air was employed for the experiments emulating the pneumatic transport of coal particles in direct-firing systems. The test rig enables an extensive variation of the most influential parameters, like the mass-flow, the velocity and the size of the particles. A linear, multi-regression analysis of the results of the experiments was carried out and the appropriate regression model enabling a determination of the mean diameter of the particles using the electrostatic signal was chosen. Based on the results of the study the electrostatic measuring technique can be used for monitoring the size of pneumatically transported particles. The appropriate regression model needs to be chosen for each particular application to describe the dependency of the acquired electrostatic signal on the influential parameters of the pneumatic transport.

Key words: *electrostatic method, rod-type sensor, particle size, pulverized coal, regression analysis*

Introduction

The electrostatic, online, continuous measuring of the characteristics of two-phase, gas-solid flow is a promising method and plenty of research has been conducted in this field in recent decades. The method can be applied in various industrial branches, like the cement and flour industries and the production of power, automotive testing, especially in coal-fired power plants for measuring the characteristics of the pneumatic transport of pulverized coal to the burners.

Recent research has mostly been concentrated on non-intrusive electrostatic sensors of the circular type, [1, 2], arc type [3, 4], and pin type [5], which were comprehensively studied numerically and experimentally. Nevertheless, the application of intrusive rod-type electrostatic sensors is attractive because of its cost effectiveness and good spatial sensitivity, especially in large, non-circular cross-sections [6, 7] typical for power plants with direct-firing systems. An

* Corresponding author, e-mail: andrej.senegacnik@fs.uni-lj.si

array of electrostatic rod-type sensors demonstrated very good performance when determining the mass-flow distribution of coal particles among burner nozzles in a full-size lignite-fired steam boiler [7] which is also very important in modelling and optimization of combustion of low rank coals [8, 9]. The electrostatic method with the appropriate statistical control scheme can be employed for the early detection and prevention of overloading the direct-firing system [10].

Last research efforts in pneumatic conveyance with deep-background review of the current state of pneumatic conveying systems and also the status of electrostatic is presented in [11]. Different research confirmed the impacts of several variables on tribocharging of powders and electrostatic method's signal [12, 13]. The properly treated signal can be employed for a determination of the mass-flow, the velocity and the mean diameter of the particles. A proportional relationship between the measured signal and the mass-flow of the particles was reported in [14]. The signal was found to be proportional to the volume concentration of the particles and the square root of the particles' velocity [15-17]. Besides this, a relation between the mass-flow and the root mean square (RMS) of the measured signal and the velocity of particles has been proposed in [18]. The efforts to correlate the electrostatic signals to particle size are reported in [19]. The phenomenon that larger particles carry higher charge [20] and that consecutively an electrostatic signal with a higher magnitude implies larger particles passing through the electrode forms the fundamental basis for the research presented in [21]. Electrostatic measurements and characterization of fine particles in diesel engine exhaust is reviewed in [22].

The most comprehensive consideration of the influential parameters with respect to the electrostatic signal was proposed in [1], introducing a non-dimensional analysis. Hence, the signals are related to the mass-flow, the velocity, the size and the electrical properties of the particles as well as to the size of the sensor. If the electrical properties, the size of the particles, the properties of the carrying gas and the size of sensor are constant during the measuring process, the relation can be significantly simplified. Such a simplified relation was successfully employed on a full-size, lignite-fired steam boiler for a determination of the coal's mass-flow distribution [7, 17] among the burner nozzles receiving the pulverized coal from a single common mill. However, testing the electrostatic measuring method in a full-size power plant is limited to the variations of the parameters that are acceptable and safe for the operation of the plant. To avoid these limitations, a test rig that allows testing over an extended span of parameters and under controlled conditions was built.

A matrix of parameter variations and a data analysis were carried out. The particles' velocity, concentration and size were kept inside the realistic operational boundaries of direct-firing systems of contemporary coal-fired boilers [9]. The regression analysis of the measured data was carried out and an appropriate regression model linking the influential variables was chosen. The Akaike information criterion, AIC_C, was used for comparing the different regression models.

Parameters influencing the electrostatic mass-flow measurement

In pneumatic transport, solid particles become electrostatically charged due to particles-to-duct friction, particles-to-particles friction, and particles-to-gas friction. The direct current (DC) that flows between the electrostatic sensor and the ground is caused by the charge being released from the particles to the sensor during their direct contact [23]. In addition, there are alternations of the current (AC) induced by the charged particles [24] bypassing the sensor. In some cases, the DC component is significant enough to enable the analysis of the acquired signals. In other cases, mostly with nonintrusive sensors, where DC component is not meaningful, the analysis of the RMS may be more appropriate.

The relation of I to the various influential parameters can be summarized as function f [1]:

$$I = f(\varepsilon, K, d_{\mathrm{m}}, v, \rho, q_{\mathrm{m}}, A_{\mathrm{s}}) \tag{1}$$

According to a non-dimensional analysis of the π theorem, the influential variables listed in eq. (1) can be grouped into four non-dimensional parameters [1]:

$$\left(\frac{I^2}{\varepsilon d^2 \rho v^4}\right) = f\left[\left(\frac{\varepsilon v}{Kd}\right), \left(\frac{d_{\mathrm{m}}^2}{A_{\mathrm{s}}}\right), \left(\frac{q_{\mathrm{m}}}{Kd\rho}\right)\right] \tag{2}$$

The previous relation is rather complex. However, many of the influential parameters can often be presumed constant, which simplifies the relation.

In many applications of pneumatic transport, the electrical permittivity, ε [Fm^{-1}], the conductivity, K [Ω^{-1}], of the particles, the density, ρ [kgm^{-3}], of the carrying gas and the cross-sectional area of the sensor, A_{s} [m^2], can be assumed to be constant. The level of electrostatic signal and cross-sectional area of the sensor facing the particles' flow are in positive correlation. Although higher levels of signals are preferred, appropriate size of sensor needs to be chosen for each particular application with respect to allowable flow restrictions.

To study the dependence of the electrostatic signal on particles' size, pulverized coal was sieved to obtain fractions with different size groups of particles. This means that the mean diameter of the particles d_{m} [μm] is constant during each test run. Equation (2) can be simplified and the mass-flow of particles q_{m} [gs^{-1}] can be expressed [7]:

$$q_{\mathrm{m}} = g\left(\frac{I^2}{v^4}\right) \tag{3}$$

For lignite particles a linear function was proposed for g [7], and it was used with success for the representation of the particles' mass-flow distribution across the duct with a large cross-section of several square meters. If a linear function is employed for g, then eq. (3) can be written:

$$I = k\sqrt{q_{\mathrm{m}} v^4} = kZ' \tag{4}$$

Due to the fact that the current, I, was measured indirectly by measuring the voltage drop, U, over the resistor, R, the following equation is used instead of eq. (4):

$$U = kZ'R = kZ \tag{5}$$

where:

$$Z = \sqrt{R^2 q_{\mathrm{m}} v^4} \tag{6}$$

The level of electrostatic signal (voltage U) is therefore linearly proportional to the variable Z, which comprises the resistance of the measuring resistor and the particles' mass-flow and velocity.

Test rig

The test rig is presented in fig. 1. The radial fan draws the air through the vertical measuring section of the main duct and then through the connecting pipes and the filter. The

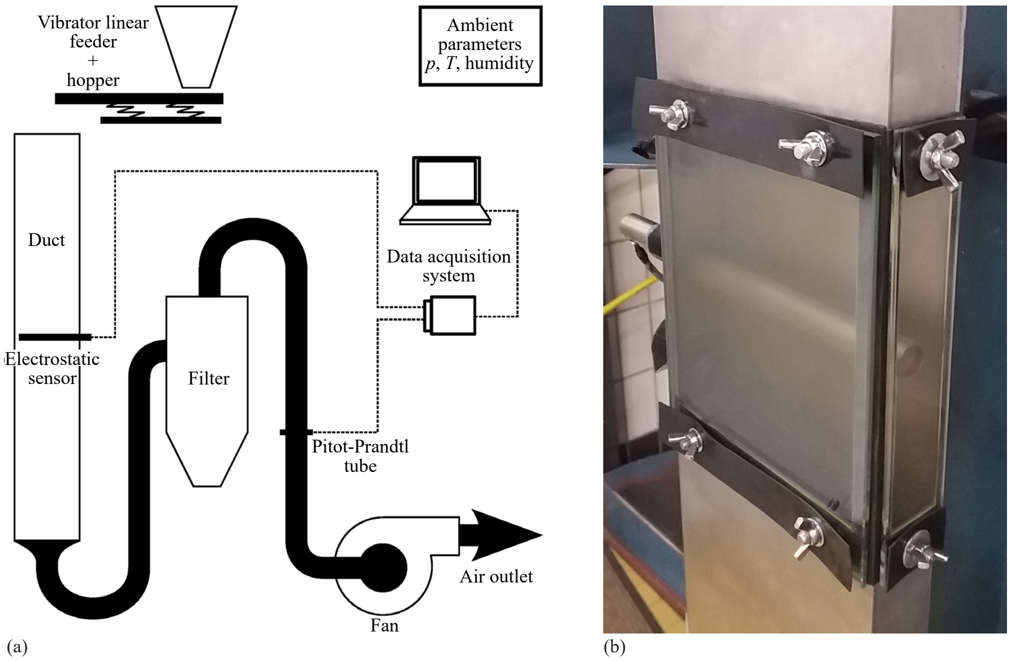

Figure 1. Test rig for experiments (a) and main duct (b)

coal particles are fed into the stream from the hopper mounted above the vibratory linear feeder. The particles are carried by the air through the main duct to the filter, where they are collected. Filtered air is then released through the exhaust. At the mid-length of the main duct, the electrostatic, intrusive rod-type sensor is mounted. Sensor rod is made of stainless steel and electrically insulated from the walls of the duct. The walls of the duct are also made of stainless steel and grounded. The electric charge that is deposited to the sensor by the particles that are colliding with the sensor causes the electric current flowing between the electrostatic sensor and the ground. In this particular case, the DC component of the current is significant enough to enable the comparison of the arithmetic means of the acquired signals.

The sensor is wired through a resistor to the ground. The voltage drops over the resistor is captured by the data-acquisition system. The mass-flow of the particles is controlled by the vibration amplitude of the vibratory linear feeder. Prior to the tests, the vibratory linear feeder was calibrated for each size fraction of particles. The frequency-controlled radial fan enables a wide range of air velocities that are measured online using a Pitot-Prandtl probe in the mid-length of a straight section of a pipe connecting the filter and the fan. Alternatively, two electrostatic sensors placed consecutively in the main duct can be used for determining the particles' velocity using the cross-correlation of the two electrostatic signals [1, 25]. By using the Pitot-Prandtl probe, the velocity of the carrying air is measured, while by using two electrostatic probes, the velocity of the particles is measured. Whenever the difference between the particles' velocity and carrying-gas's velocity can be neglected, both methods can be employed. In this case a Pitot-Prandtl probe is chosen to minimize the flow restrictions and disturbances in the measuring section of the main duct.

The ambient air pressure, temperature and humidity were recorded during the test runs.

The diameter and the length of the rod-type electrostatic sensor made of stainless steel are 21.3 mm and 200 mm, respectively. The main duct is 2 m long with a cross-section of

0.01 m^2 (0.050 m × 0.200 m). The hopper can hold 15 dm^3 of pulverized coal. The filter retains particles above 5 μm in diameter.

The voltage drop over a 1-MΩ measuring resistor (electrostatic signal) was recorded using a NI-cRIO platform and a NI 9205 module with a sampling frequency of 1000 Hz. The highly fluctuating voltage time series were smoothed by calculating the moving averages of five means of batches, each containing 1000 readings.

Pulverized coal

The pulverized coal used for the experiments was obtained from a commercial coal-fired power plant. It was extracted from the duct leading to the burner at the classifier outlet using an isokinetic sampling kit [7]. The mass composition of the pulverized coal is summarized in tab. 1.

Table 1. Mass composition of the pulverized coal

Moisture	Ash	C	H	N	O	S
7.63%	20.91%	40.62%	3.25%	0.90%	25.18%	1.51%

Because the goal of the research was to isolate the effect of the particle diameters on the electrostatic signal, the pulverized coal was sieved according to a standard procedure [26] into four particle size fractions of approximately the same weight. The mean diameter, d_m, for each size fraction was established according to the Rosin-Rammler distribution.

d > 250 μm $\quad$ d_m = 600 μm
125 μm < d <250 μm $\quad$ d_m = 178 μm
45 μm < d <125 μm $\quad$ d_m = 82 μm
d < 45 μm $\quad$ d_m = 31 μm

The coarser three fractions were used for the testing. The fraction d < 45 μm was not tested because it could not be adequately fed with the vibratory feeder. The particles were too cohesive, according to the Geldart classification.

It should be noted that moisture content has a significant effect on the level of the electrostatic signal because the electrical properties of the particles depend on the moisture content. Adsorbed moisture on the surface of the particles increases the conductivity and intensifies the charge-relaxation phenomenon [27]. Consequently, lower electrostatic signals can be observed at higher moisture contents. The moisture-content effect is more evident with smaller particle sizes due to the higher surface-to-mass ratio.

Figure 2 shows the effect of increased moisture on the electrostatic signal. The solid line represents the electrostatic signal induced by the pulverized coal with 8% moisture, while the dotted line represents the electrostatic signal induced by the same fraction of pulverized coal that was exposed to ambient air for two days and had a moisture content of 14%. To emulate the original moisture content in pulverized coal prepared for firing, tab. 1, and to fulfill the condition of constant electrical properties in section *Parameters influencing the electrostatic mass-flow measurement*, the coal was dried prior to each test run to a moisture content of 8%. In the subsequent analysis only the results obtained with dried samples are considered.

Experimental procedure

The vibratory-linear feeder was calibrated for three particles' size fractions of pulverized coal at different settings of feeder vibrating amplitudes. To verify the repeatability, six

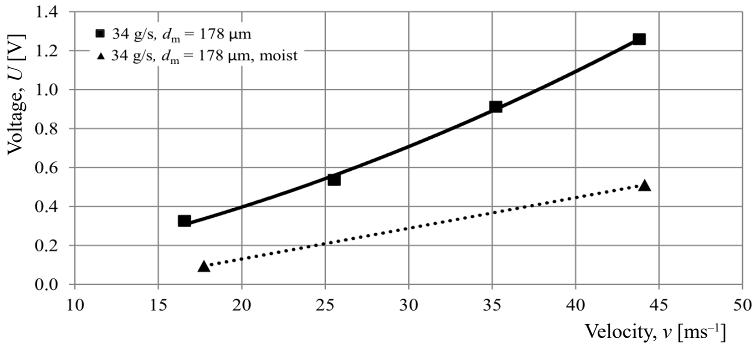

Figure 2. Effect of the moisture content on the electrostatic signal

runs were carried out for each setting of the feeder and for each size fraction. During the vibratory operation of the feeder, weight of coal particles was measured by means of the electronic bench scale connected to the computer. The minimal, the maximal and the mean mass-flows were identified. The absolute value of the maximum relative difference between the mean and the minimal or the mean and the maximal mass-flows is presented as a red curve on fig. 3. For example, the uncertainty of feeding for 110 g/s is ±11% (12.1 g/s).

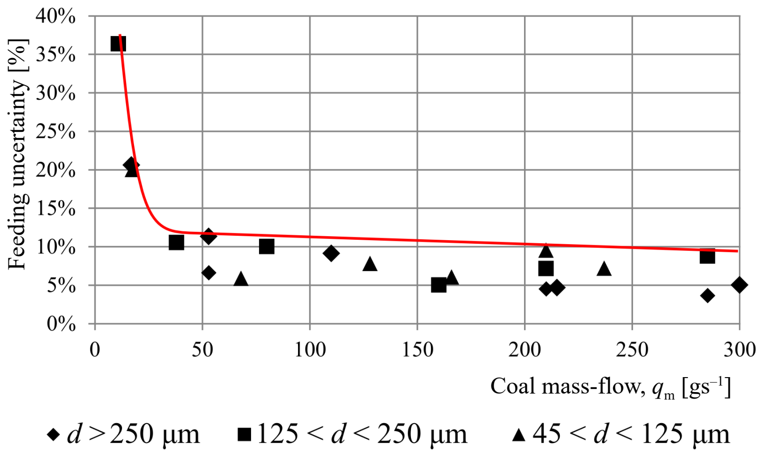

Figure 3. Scatter of the calibration results

Figure 4 shows an example of the electrostatic signal, *U,* (raw and smoothed voltage) and the velocity, *v,* recorded during one of the test runs. For each test run, approximately 9 kg of pulverized coal was used. The mean values of the signal and velocity that were recorded during stabile intervals (*e. g.*, between 30 seconds and 70 seconds in fig. 4) of each test run were used for the analysis. The lead-in and lead-out intervals were disregarded.

For the pneumatic transport of the pulverized coal in direct-firing systems, the recommended upper concentration limit is about 0.80 kg of pulverized coal per 1 kg of carrying gas [28]. All the test runs were carried out below this limit. The highest concentration of 0.75 kg of coal per 1 kg of carrying air was achieved during the test run with a mass-flow of 120 g/s and a velocity of 14 m/s.

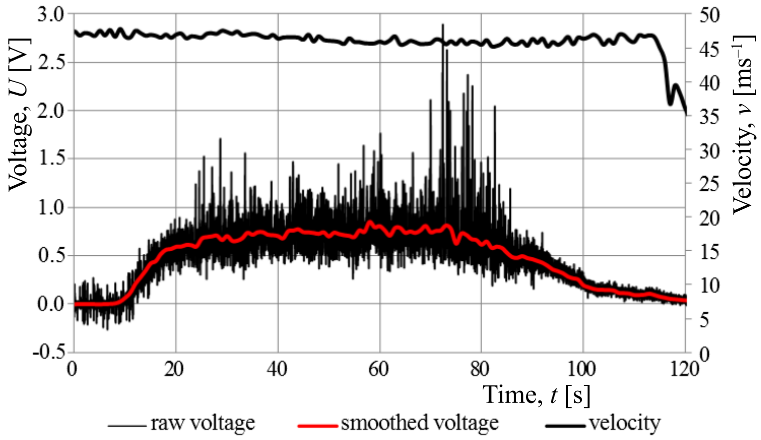

Figure 4. Recording of the raw and the smoothed voltage, *U*, and the velocity, *v*, during a test run with the particle size d_m = 600 μm, mass-flow 110 g/s, and mean velocity, *v*, of the carrying gas 46.2 m/s

To maintain smooth pneumatic transport, the velocities in the ducts of direct-firing systems are normally higher than 20 m/s. The majority of the test runs were conducted above this velocity.

The dependencies of the electrostatic signals on the particles' mass-flow, velocity and size are presented in fig. 5.

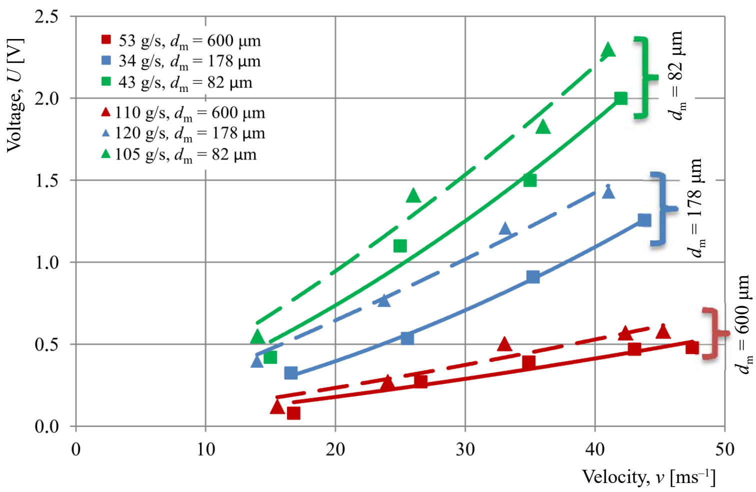

Figure 5. Electrostatic signal in relation to particles' size, velocity and mass-flow

They are in accordance with [16], where a lower electrostatic signal was reported for the coarser particles. The same effect was observed during electrostatic measurements carried out in a real power plant [7]. The electric charge that can be deposited on the electrostatic probe is positioned on the surface of the particles. Assuming the particles have a constant surface-charge density, larger particles can carry higher charges than smaller particles [20]. This is also the reason why AC component of the electrostatic signal (induction) is in positive correlation with mean diameter of particles [21]. But at the same time, assuming the same total mass of particles, total surface of smaller particles is larger than total surface of larger particles. This is why DC component of the electrostatic signal, caused by direct contact of particles and sensor, is in positive correlation with total surface of particles *i. e.* in negative correlation with the mean diameter of particles.

A higher mass-flow of particles and a higher velocity induced higher electrostatic signals. The same observations were reported in [1, 7, 23].

Regression analysis

Figure 6 shows the variable Z as a function of the electrostatic signal (voltage U) and the mean diameter of the particles, d_m. The variable Z was calculated according to eq. (6) for each combination of the mass-flow, velocity and mean diameter of the particles. The linear-approximation functions, as proposed in eq. (5), were determined for each size fraction of particles. The functions intercept the origin of the co-ordinate system. The high values of the determination coefficients, R^2, show that the functions statistically clearly describe the relations between the variables Z and the measured voltages, U, which confirms the findings of [7].

It is evident that the coefficients, k, eq. (5), depend on the mean diameters of the particles' size fractions that were used for the respective test runs and that k can be used for the detection of the mean diameter variations:

$$d_m = 82\,\mu\text{m} \quad \rightarrow \quad k = \frac{1}{6.04 \cdot 10^9} \frac{\text{V}}{\left(\text{g}\,\Omega^2\text{m}^4\text{s}^{-5}\right)^{0.5}}$$

$$d_m = 178\,\mu\text{m} \quad \rightarrow \quad k = \frac{1}{9.89 \cdot 10^9} \frac{\text{V}}{\left(\text{g}\,\Omega^2\text{m}^4\text{s}^{-5}\right)^{0.5}}$$

$$d_m = 600\,\mu\text{m} \quad \rightarrow \quad k = \frac{1}{3.11 \cdot 10^{10}} \frac{\text{V}}{\left(\text{g}\,\Omega^2\text{m}^4\text{s}^{-5}\right)^{0.5}}$$

According to fig. 6 particles' size fractions with smaller mean diameters produce higher DC components of electrostatic signals at equal values of the variable Z (combined effect of mass-flow and velocity of particles on electrostatic signal). The goal of multi-regression analysis is to find the appropriate computational model to relate the electrostatic signal U, the variable Z and the mean diameter of the particles' size fraction d_m using the results of the experiments:

$$U \approx f\left(Z, d_m\right) \tag{7}$$

Many models can be used to relate U, Z, and d_m, but the balance between the accuracy and the complexity of the model should be kept in mind. The multi-regression adjusted determination coefficient, R^2_{adj}, due to its extensive use [29], and the corrected Akaike information criterion AIC_C, due to its applicability for a small number of data points [30] are used in this study.

Table 2 comprises the results of the evaluation of two sets of linear models. In one of the sets, the functions are forced to intercept the origin of the co-ordinate system. The values of R^2_{adj} lie between zero and one, with higher values indicating better-fitted models. In contrast, lower values of AIC_C indicate better-fitted models. As expected, the two criteria rate the con-

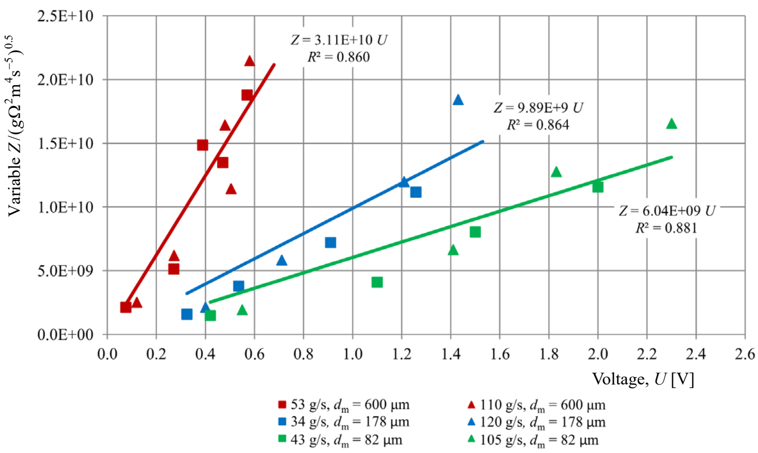

Figure 6. Variable *Z* as function of the voltage, *U*, and the mean diameter of the particles

sidered models $i = 1,2,\ldots,n$ differently. AIC_C was chosen to be the decisive criterion because it deals with the trade-off between the goodness of fit of the model and the simplicity of the model, while R^2_adj only takes into account the goodness of fit. Model 17 was chosen, eq. (8), according to the AIC_C criterion, tab. 2.

Table 2. Comparison of the regression models

	i	Model	R^2_adj	AICc
Without intercept in origin	1	$\beta_0 + \beta_1 Z + \beta_2 d_\mathrm{m} + \beta_3 Z d_\mathrm{m} + \beta_4 Z^2 + \beta_5 d_\mathrm{m}^2 + \beta_6 Z^2 d_\mathrm{m} + \beta_7 d_\mathrm{m}^2 Z$	0.962	18.278
	2	$\beta_0 + \beta_1 Z + \beta_2 d_\mathrm{m} + \beta_3 Z d_\mathrm{m} + \beta_4 Z^2 + \beta_5 d_\mathrm{m}^2$	0.943	–2.137
	3	$\beta_0 + \beta_1 Z + \beta_2 d_\mathrm{m} + \beta_3 Z^2 + \beta_4 d_\mathrm{m}^2$	0.894	–0.627
	4	$\beta_0 + \beta_1 Z + \beta_2 d_\mathrm{m} + \beta_3 Z d_\mathrm{m} + \beta_4 Z^2$	0.934	–7.283
	5	$\beta_0 + \beta_1 Z + \beta_2 d_\mathrm{m} + \beta_3 Z d_\mathrm{m}$	0.933	–12.093
	6	$\beta_0 + \beta_1 Z + \beta_2 d_\mathrm{m}$	0.899	–10.013
	7	$\beta_0 + \beta_1 Z$	0.702	2.339
	8	$\beta_0 + \beta_1 d_\mathrm{m}$	0.058	18.430
	9	$\beta_0 Z^{\beta 1} d_\mathrm{m}^{\beta 2}$	0.947	1.474
	10	$\beta_0\, Z^{\beta 1}\, e^{\beta 2}$	0.831	17.554
	11	$\beta_0\, e^{\beta 1}\, d_\mathrm{m}{}^{\beta 2}$	0.954	–0.482
	12	$e^{\beta 0 + \beta 1 d\mathrm{m} + \beta 2 Z}$	0.831	17.552
Intercept in origin	13	$0 + \beta_1 Z + \beta_2 d_\mathrm{m} + \beta_3 Z d_\mathrm{m} + \beta_4 Z^2 + \beta_5 d_\mathrm{m}^2 + \beta_6 Z^2 d_\mathrm{m} + \beta_7 d_\mathrm{m}^2 Z$	0.990	0.543
	14	$0 + \beta_1 Z + \beta_2 d_\mathrm{m} + \beta_3 Z d_\mathrm{m} + \beta_4 Z^2 + \beta_5 d_\mathrm{m}^2$	0.979	–6.189
	15	$0 + \beta_1 Z + \beta_2 d_\mathrm{m} + \beta_3 Z^2 + \beta_4 d_\mathrm{m}^2$	0.962	–2.778
	16	$0 + \beta_1 Z + \beta_2 d_\mathrm{m} + \beta_3 Z d_\mathrm{m} + \beta_4 Z^2$	0.981	–12.579
	17	$\boldsymbol{0 + \beta_1 Z + \beta_2 d_\mathrm{m} + \beta_3 Z d_\mathrm{m}}$	**0.976**	**–12.801**
	18	$0 + \beta_1 Z + \beta_2 d_\mathrm{m}$	0.932	–0.965
	19	$0 + \beta_1 Z$	0.913	0.171
	20	$0 + \beta_2 d_\mathrm{m}$	0.274	29.895

The chosen model was further checked using the traditional normal quantile-quantile QQ plot, fig. 7. The solid line represents the results of the model and the circles represents the measured data. The dashed lines designate the 95% confidence interval.

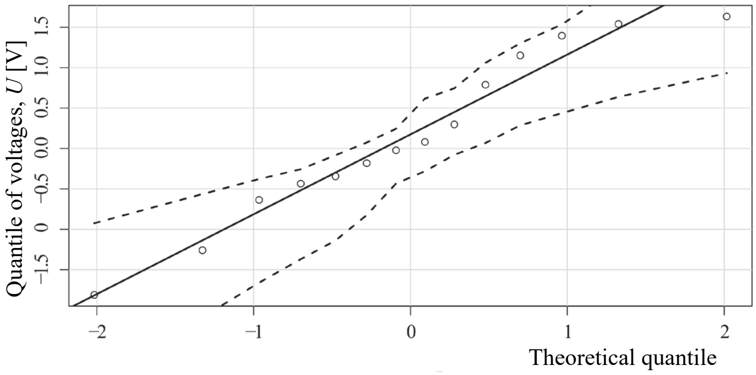

Figure 7. Quantile-quantile plot for eq. (8) and the measured data

The equation representing the chosen model that was derived according to the results of the tests and relates the electrostatic signal U to Z and d_m is:

$$U = 7.144 \cdot 10^{-11} Z + 1.144 \cdot 10^{-4} d_m - 6.758 \cdot 10^{-14} Z d_m \tag{8}$$

The model can be employed either for the mass-flow q_m or for the d_m computation.

Figure 8 shows the results of the measurements (blue dots) and of the computations according to eq. (8) (mesh surface).

Metrologic evaluation of the mass-flow regression model [31, 32] shows that the absolute standard uncertainty of the regression model for voltage is ±0.11 V (±8.34 g/s). Relative standard uncertainty of modeled coal mass-flow in the duct equals ±19.2% (±21.1 g/s at mass-flow 110 g/s).

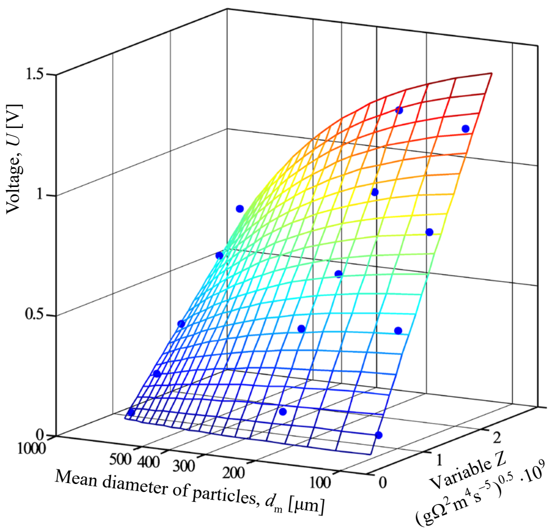

Figure 8. Approximation model of the voltage, *U*, as a function of the variables *Z* and d_m (*for color image see journal web site*)

Practical application

The goal of the study was to determine the applicability of the electrostatic measuring method for monitoring the deterioration of coal-milling performance in the direct-firing systems of conventional power plants fired with low-rank coal. Due to the wear of vital parts of the direct-firing system, the deterioration of milling performance gradually progresses. The mean diameter of the coal particles gradually increases and this affects the quality of the combustion process. Consequently, the emission of harmful gases like CO and NO_x increases and the boiler efficiency decreases. The speed of deterioration of the milling process is different for each particular boiler. It depends on the composition of the coal, the material of impact plates and inner linings of mills, average load of mills, average temperature in mills *etc*. In general, the condition of each mill of one particular direct firing system is different due to different number of operating hours and different operating conditions. It is therefore important that the boiler operators detect the deterioration of milling and pinpoint which particular mill needs maintenance. For this particular application it is more important to be able to detect the deterioration of milling quality than to know the precise absolute mean diameter of particles.

Currently, isokinetic sampling and laser-based measuring methods are the most widely used for periodic monitoring the milling process. These methods involve a lot of personnel and are time consuming. They are also not suitable for continuous monitoring and do not provide the operators with continuous online information about the milling performance.

The electrostatic measuring technique in connection with rod-type intrusive sensors is, on the other hand, very suitable for continuous monitoring. In [25] the practical application of the same technique for monitoring the coal distribution between burner nozzles, velocity of pulverized coal and early detecting the mill overload is described.

It should be noted that the relation represented by eq. (8) is valid for the specific coal and specific test rig used for the laboratory experiment. A similar model can be derived for any other application involving dilute pneumatic transport. The DC level of electrostatic signal depends, besides on the influential parameters listed in eq. (1), on other stochastic parameters like mechanical processes and configuration and materials of piping upstream the electrostatic measurement. This is the main reason why each particular application needs calibration. For the calibration, *i. e.* for establishing the relations between the electrostatic signal and the velocity, mass-flow and mean diameter of the particles, any of the conventional off-line techniques may be used. In applications where knowing the mean diameter of the particles is essential, the appropriate calibration technique must be chosen to ensure the required accuracy.

Conclusions

The results of the study prove that, the electrostatic measuring technique is applicable for measuring mean diameters of particles in dilute pneumatic transport. The tests were carried out with pulverized coal, but the technique may also be applied in other applications involving dilute pneumatic transport. Depending on chemical composition of particles and other parameters, some applications may not be suitable for this technique due to unsufficiently charged particles. Special attention needs to be payed to moisture content when hygroscopic particles are measured.

The smoothed electrostatic signals (moving average) were used to differentiate between different particles' size fractions. Electrostatic signal, velocity and mass-flow of particles need to be measured simultaneously for the determination of mean diameter of particles. Variable Z was introduced to isolate the effects of mass-flow and velocity from the particle-size effect on the level of electrostatic signals. Negative correlation was found between the level of electrostatic signals and mean particles' size. In other words, the same mass-flow of smaller particles induce higher levels of electrostatic signals than those of larger particles.

Due to the fact that electrostatic charge carried by particles depends on many stochastic parameters, the universal regression model does not exist. The unique regression model needs to be developed for each particular application. Conventional off-line methods for mass-flow, velocity and particle size measurements may be employed for establishing the required relations. The accuracy of the regression model depends on the accuracy of the calibration techniques.

Nomenclature

d_m – mean diameter of the particles, [μm]
f, g – function, [–]
I – electrical current, [A]
k – coefficient, [V $(g\Omega^2m^4s^{-5})^{-0.5}$]
q_m – mass-flow of the particles, [gs^{-1}]
R – resistance, [Ω]
U – voltage, [V]
v – velocity of particles in the vicinity of the sensor, [m s^{-1}]
Z – dependent variable of R, q_m, v, [$(g\Omega^2m^4s^{-5})^{-0.5}$]

References

[1] Zhang, J., Air-Solids Flow Measurement Using Electrostatic Techniques, in: *Electrostatics*, (Ed. Canbolat, H.,), InTech, Rijeka, Croatia, 2012, pp. 61-80
[2] Gajewski, J. B., Electrostatic Nonintrusive Method for Measuring the Electric Charge, Mass Flow Rate, and Velocity of Particulates in the Two-Phase Gas-Solid Pipe Flows – Its Only or as Many as 50 Years of Historical Evolution, *IEEE Trans. Ind. Appl.*, *44* (2008), 5, pp. 1418-1430
[3] Qian, X., *et al*., Quantitative Characterization of Pulverized Coal and Biomass-Coal Blends in Pneumatic Conveying Pipelines Using Electrostatic Sensor Arrays and Data Fusion Techniques, *Meas. Sci. Technol.*, *23* (2012), 8, pp. 1-13
[4] Xu, C., *et al.*, Investigations into Sensing Characteristics of Electrostatic Sensor Arrays through Computational Modelling and Practical Experimentation, *J. Electrostat.*, *70* (2012), 1, pp. 60-71
[5] Rahmat, M. F., Kamaruddin, N. S., An Electrodynamic Sensor for Electrostatic Charge Measurement, *Int. J. Smart Sens. Intell. Syst.*, *2* (2009), 2, pp. 200-212
[6] Krabicka, J., Yan, Y., Finite-Element Modeling of Electrostatic Sensors for the Flow Measurement of Particles in Pneumatic Pipelines, *IEEE Trans. Instrum. Meas.*, *58* (2009), 8, pp. 2730-2736
[7] Jurjevčič, B., *et al.*, The Characterization of Pulverized-Coal Pneumatic Transport Using an Array of Intrusive Electrostatic Sensors, *IEEE Trans. Instrum. Meas.*, *64* (2015), 12, pp. 3434-3443
[8] Živković, G., *et al*., Numerical Simulation of the Influence of Stationary Louver and Coal Particle Size on Distribution of Pulverized Coal to the Feed Ducts of a Power Plant Burner, *Thermal Science*, *13* (2009), 4, pp. 79-90
[9] Belošević, S. V., *et al*., Modeling of Pulverized Coal Combustion for In-Furnace NO_x Reduction and Flame Control, *Thermal Science*, *21* (2017), Suppl. 3, pp. S597-S615
[10] Jurjevčič, B., *et al*. A Surveillance of Direct-Firing System for Pulverized-Coal Using Statistically Treated Signals from Intrusive Electrostatic Sensors, *Journal of Mechanical Engineering*, *63* (2017) 4, pp. 265-274
[11] Klinzig, G. E., A Review of Pneumatic Conveying Status, Advances and Projections, *Powder Technology*, *333* (2018), June, pp. 78-90
[12] Taghavivand, M., *et al*., Study of Electrostatic Charging of Single Particles During Pneumatic Conveying, *Powder Technology*, *355* (2019), Oct., pp. 242-250
[13] Saleh, K., *et al*., Relevant Parameters Involved in Tribocharging of Powders During Dilute Phase Pneumatic Transport, *Chemical Engineering Research and Design*, *89* (2011), 12, pp. 2582-2597
[14] Matsusaka, S., Masuda, H., Simultaneous Measurement of Mass Flow Rate and Charge-to-Mass Ratio of Particles in Gas-Solids Pipe Flow, *Chem. Eng. Sci., 61* (2006), 7, pp. 2254-2261
[15] Carter, R. M., *et al*. On-Line Measurement of Particle Size Distribution and Mass Flow Rate of Particles in a Pneumatic Suspension Using Combined Imaging and Electrostatic Sensors, *Flow Meas. Instrum., 16* (2005), 5, pp. 309-314
[16] Zhang, J., *et al.*, Analyses of Characteristics of Ring-Shaped Electrostatic Meter, *Chem. Eng. Commun., 197* (2009), 2, pp. 192-203
[17] Despotović, Ž., V., Some Experiences in the Exploitation of Triboelectric Sensors for Measuring Concentration of Particulate Matter on Thermal Power Plants, *Infoteh-Jahorina*, *12* (2013), Mar., pp. 1118-1124
[18] Qian, X., *et al*., Measurement of the Mass Flow Distribution of Pulverized Coal in Primary Air Pipes Using Electrostatic Sensing Techniques, *Proceedings*, 2nd IEEE International Instrumentation and Measurement Technology Conference, Taipei, Thailand, 2016, pp. 1-5
[19] Coulthard, J., *et al*., Online Pulverized-Fuel Monitoring at Methil Power Station, *Power Engineering Journal, 11* (1997), 1, pp. 27-30
[20] Rodrigues, M. V., *et al*., Measurement of the Electrostatic Charge in Airborne Particles: II-Particle Charge Distribution of Different Aerosols, *Brazilian Journal of Chemical Engineering, 23* (2006), 1, pp. 125-133

[21] Zhang, J., *et al*., On-Line Continuous Measurement of Particle Size Using Electrostatic Sensors, *Powder Technology, 135-136* (2003), Oct., pp. 164-168
[22] Petrović, V. S., *et al*., The Possibilities for Measurement and Characterization of Diesel Engine Fine Particles, *Thermal Science, 15* (2011), 4, pp. 915-938
[23] Woodhead, S. R., *et al*., Electrostatic Sensors Applied to the Measurement of Electric Charge Transfer in Gas-Solids Pipelines, *Proceedings*, Sensors and their Applications, University of Greenwich, Medway, UK, 2005, Vol. 15, pp. 108-112
[24] Peng, L., *et. al.*, Characterization of Electrostatic Sensors for Flow Measurement of Particulate Solids in Square-Shaped Pneumatic Conveying Pipelines, *Sensors Actuators A Phys*., *141* (2008), 1, pp. 59-67
[25] Kuštrin, I., Lenart, J., Electrostatic Sensors on a Lignite – Fired Boiler for Continuously Monitoring the Distribution and Velocity of Pulverized Coal, *VGB Powertech*, *95* (2015), 7, pp. 33-37
[26] ***, ASTM - D197 − 87, 'Standard Test Method for Sampling and Fineness Test of Pulverized Coal', 2012
[27] Saleh, K., *et al.*, Relevant Parameters Involved in Tribocharging of Powders During Dilute Phase Pneumatic Transport, *Chem. Eng. Res. Des.*, *89* (2011), 12, pp. 2582-2597
[28] Gulič, M., *et al.*, *Proračun Ventilatorskih Mlinova*, (Fan-impact mill calculations – in Serbian), Udruženi, Belgrade, Serbia, 1982
[29] Soong, T. T., *Fundamentals of Probability and Statistics for engineers*, Wiley, New York, USA, 2004
[30] Hurvich, C. M., Tsai, C. L., Regression and Time Series Model Selection in Small Samples, *Biometrika, 76* (1989), 2, pp. 297-307
[31] Degiuli, N., *et al.,* Causes of Sampling Measurement Uncertainties when Determining the Particle Concentration in a Gaseous Environment, *J. Mech. Eng.*, *53* (2007), 5, pp. 297-309
[32] ***, Joint Committee for Guides in Metrology, JCGM 100:2008 Evaluation of Measurement Data – Guide to the Expression of Uncertainty in Measurement, Corrected Version 2010, 2010

Paper submitted: Apryl 17, 2019
Paper revised: August 8, 2019
Paper accepted: August 13, 2019